Theor Chem Acc (1999) 101:343–351
DOI 10.1007/s00214980m162

Theoretical Chemistry Accounts

Regular article

A theoretical study on the first ionic states of vinyl fluoride, vinyl chloride, trifluoroethylene, and trichloroethylene with an analysis of the vibrational structures of the photoelectron spectra

Kouichi Takeshita

Faculty of Bioindustry, Tokyo University of Agriculture, Abashiri, Hokkaido 099-2493, Japan

Received: 11 September 1998 / Accepted: 13 October 1998 / Published online: 1 February 1999

Abstract. Ab initio calculations have been performed to study the molecular structures and the vibrational levels of the first ionic states of vinyl fluoride, vinyl chloride, trifluoroethylene, and trichloroethylene. The equilibrium molecular structures and vibrational modes of these states are presented. The theoretical ionization intensity curves including the vibrational structures are also presented and compared with the photoelectron spectra.

Key words: Vinyl fluoride – Vinyl chloride – Trifluoroethylene – Trichloroethylene – Restricted Hartree–Fock gradient – molecular structure vibrational analysis

1 Introduction

The electronic configurations of the ground states of vinyl fluoride (C_2H_3F), vinyl chloride (C_2H_3Cl), trifluoroethylene (C_2HF_3), and trichloroethylene (C_2HCl_3) are represented by $\ldots(10a')^2\,(2a'')^2$, $\ldots(13a')^2\,(3a'')^2$, $\ldots(16a')^2\,(4a'')^2$, and $\ldots(25a')^2\,(7a'')^2$ with the point group C_s, respectively. The electronic configurations of the valence electrons of C_2H_3F and C_2H_3Cl have the same structure, and those of C_2HF_3 and C_2HCl_3 also have the same structure. For all molecules, the first ionic state is the $^2A''$ state, where an electron is removed from the highest occupied a'' molecular orbital. The highest occupied orbital has a π-bond character.

Several photoelectron spectroscopic investigations have been published by many different researchers [1–5]. It has been shown that the first band has vibrational structure and that the upper bands have more complicated forms.

Theoretical studies of the photoelectron spectra have been reported by some researchers [3–6]. Heaton and El-Talbi [6] obtained the molecular structures of the ground states of fluorinated ethylenes and the vertical ionization energies in order to assign the electronic states.

As far as we are aware, there is no theoretical study of the molecular structures and vibrational levels of the ionic states. There is also no theoretical study of the vibrational structure of the photoelectron spectrum. In this paper we examine theoretically the molecular structures and vibrational levels of the first ionic states.

Within the framework of the adiabatic approximation and the harmonic oscillator approximation, we calculated the harmonic force constant matrix elements over varibales of the totally symmetric distortion and the vibrational frequencies of the totally symmetric modes. We have obtained approximate theoretical intensity curves using the Franck–Condon factor (FCF), which is calculated by taking the square of the overlap integrals between the vibrational wavefunction of the ground state and that of the ionic state. Based on these calculations, we discuss the assignment of the vibrational structure of the spectrum compared with the photoelectron spectrum.

2 Method of calculation

We used the split-valence-type basis sets of the MIDI-4-type prepared by Tatewaki and coworkers [7, 8]. These are augmented by one *p*-type polarization function for H and one *d*-type polarization function of C, F, and Cl. The exponents of the polarization functions of H, C, F, and Cl are 0.68, 0.61, 1.50 and 0.56, respectively.

The gradient technique for Roothaan's restricted Hartree–Fock (RHF) method was applied to find the optimum molecular structures of the ground and ionic states.

The normal vibrational calculation of the totally symmetric modes was done by means of the gradient technique with the RHF wave function. We placed some restrictions on the calculation of the FCF as follows: only vibrational transitions between the zero-point vibrational level of the ground state and the totally symmetric modes of the ionic state were allowed. The methods of calculation of the FCF and the theoretical intensity curve were the same as we used in a previous paper [9].

The single and double excitations configuration interaction (SDCI) method was used to obtain more accurate ionization energies. We used a single reference configuration of the RHF wave function of the respective state. In the SDCI method, singly and doubly excited configuration state functions were generated where the inner shells were kept frozen.

In the calculation of the theoretical intensity curve, we used the 0-0 ionization energy obtained by the SDCI method.

This work was carried out using the computer program system GRAMOL [10] for the gradient technique and the calculation of normal modes, and ALCHEMY II [11–13] for the CI calculations.

3 Results and discussion

The optimized geometrical parameters of the ground and first ionic states are listed in Table 1, while Table 2 gives the vertical and adiabatic ionization energies at the SCF and SDCI levels. The energy lowering of the adiabatic ionization energy compared with the vertical ionization energy is also given in Table 2. The 0-0 ionization energies and the FCFs of the 0-0 transitions are included in Table 2. The observed 0-0 ionization energies [3, 4] of C_2H_3F, C_2H_3Cl, C_2HF_3, and C_2HCl_3 are 10.36, 10.0, 10.14, and 9.48 eV, respectively. In the SDCI calculations, the weights of the reference function of the $^2A''$ state of C_2H_3F, C_2H_3Cl, C_2HF_3, and C_2HCl_3 are 90, 88, 87, and 84%, respectively, at the optimized geometry.

The vibrational frequencies of the ground and ionic states are listed in Tables 3–6. The frequencies are arranged in order of magnitude. Each vibrational mode is

Table 1. Optimized molecular structure[a]

	C=C	C–X[b]	C–H_1[c]	C–H_2[c]	C–H_3[c]	C=C–X[b]	C=C–H_1[c]	C=C–H_2[c]	C=C–H_3[c]
C_2H_3F									
$^1A'$	1.312	1.325	1.081	1.082	1.081	122.51	125.29	121.31	119.51
$^2A''$	1.402	1.249	1.087	1.085	1.083	119.65	124.53	119.77	119.43
C_2H_3Cl									
$^1A'$	1.315	1.742	1.080	1.082	1.083	123.12	124.03	122.14	119.51
$^2A''$	1.402	1.645	1.086	1.084	1.084	122.13	121.19	120.80	119.41
	C=C	C–X_1[b,d]	C–X_2[b,d]	C–X_3[b,d]	C–H	C=C–X_1[b,d]	C=C–X_2[b,d]	C=C–X_3[b,d]	C=C–H
C_2HF_3									
$^1A'$	1.307	1.294	1.299	1.323	1.076	125.59	122.87	120.95	122.64
$^2A''$	1.405	1.236	1.238	1.259	1.083	122.29	120.70	117.58	122.45
C_2HCl_3									
$^1A'$	1.317	1.721	1.733	1.724	1.078	124.77	120.10	124.23	120.75
$^2A''$	1.410	1.666	1.669	1.652	1.083	122.46	118.11	123.66	118.64

[a] Bond lengths in angstroms, angles in degrees
[b] X = F or Cl
[c] The compositions of H_1, H_2, and H_3 are as follows: H_2 and H_3 combine with the same carbon; H_1 and H_3 are located on the same side
[d] The compositions of X_1, X_2, and X_3 are as follows: X_2 and X_3 combine with the same carbon; X_1 and X_3 are located on the same side

Table 2. Ionization energies (*IE*) of the $^2A''$ state[a]

Molecule	Vertical IE		Adiabatic IE		(Vertical IE-Adiabatic IE)		0-0 transition	
	SCF	SDCI	SCF	SDCI	SCF	SDCI	0-0 IE	FCF
C_2H_3F	9.22	9.99	8.83	9.60	0.39	0.39	9.60	0.141
C_2H_3Cl	9.11	9.79	8.76	9.41	0.35	0.38	9.41	0.135
C_2HF_3	9.55	9.91	8.90	9.35	0.65	0.56	9.36	0.041
C_2HCl_3	9.06	9.39	8.65	8.96	0.41	0.43	8.96	0.071

[a] Total energies of the $^1A'$state of C_2H_3F, C_2HF_3, C_2H_3Cl, and C_2HCl_3 are −176.697201, −374.187023, −536.360465, and −1453.171311, respectively at the RHF level. Total energies of the $^1A'$ state of C_2H_3F, C_2HF_3, C_2H_3Cl, and C_2HCl_3 are −177.126235, −374.898295, −536.748871, and −1453.760361, respectively at the SDCI level

Table 3. Vibrational frequencies (cm^{-1}) and potentital energy distributions (*PED*) of C_2H_3F[a]

State	Mode	Vibrational frequency	PED (%)
$^1A'$	ν_1	3434	C–H_3(56), C–H_2 (39), C–H_1 (5)
	ν_2	3395	C–H_1 (91), C–H_2 (7)
	ν_3	3333	C–H_2 (53), C–H_3 (43)
	ν_4	1879	C=C (73), C–F (9), C=C–H_1 (9), C=C–H_2 (5)
	ν_5	1518	C=C–H_3 (45), C=C–H_1 (32), C=C–H_2 (15), C–F (8)
	ν_6	1428	C=C–H_1 (68), C=C–H_2 (17), C=C (12)
	ν_7	1273	C–F (44), C=C–H_2 (25), C=C–F (16), C=C–H_3 (14)
	ν_8	1023	C=C–H_3 (37), C=C–H_2 (29), C–F (27)
	ν_9	519	C=C–F (56), C=C–H_1 (18), C=C–H_2 (14), C=C–H_3 (12)
$^2A''$	ν_1	3450	C–H_3 (56), C–H_2 (43)
	ν_2	3380	C–H_1 (97)
	ν_3	3314	C–H_2 (55), C–H_3 (43)
	ν_4	1737	C=C (34), C–F (32), C=C–H_1 (27), C=C–H_2 (7)
	ν_5	1554	C=C–H_3 (52), C=C–H_2 (18), C–F (17)
	ν_6	1413	C=C–H_1 (52), C–F (41)
	ν_7	1337	C=C (38), C=C–H_2 (26), C=C–H_1 (16), C=C–F (12)
	ν_8	1059	C=C–H_3 (43), C=C– H_2 (35), C=C (10), C–F (10)
	ν_9	521	C=C–F (57), C=C–H_1 (19), C=C–H_2 (12), C=C–H_3 (11)

[a] The values of the PED (%) over 5% are listed

Table 4. Vibrational frequencies (cm^{-1}) and (PED) of C_2H_3Cl[a]

State	Mode	Vibrational frequency[b]	PED (%)
$^1A'$	ν_1	3420	C—H_2 (49), C—H_3 (43), C—H_1 (8)
	ν_2	3395	C—H_1 (88), C—H_3 (9)
	ν_3	3322	C—H_3 (56), C—H_2 (41)
	ν_4	1822	C=C(79), C=C—H_2 (7), C=C—H_3 (6)
	ν_5	1501	C=C—H_3 (44), C=C—H_2 (32), C=C (13), C=C—H_1 (8)
	ν_6	1390	C=C—H_1 (76), C=C—H_2 (12), C=C—H_3 (5)
	ν_7	1117	C=C—H_2 (43), C=C—H_3 (42), C=C—Cl(7), C—Cl(5)
	ν_8	760	C—Cl (71), C=C—H_3 (8), C=C—Cl(7), C=C—H_1 (7), C=C—H_2 (6)
	ν_9	423	C=C—Cl (70), C=C—H_1 (14), C=C—H_2 (7), C=C—H_3 (6)
$^2A''$	ν_1	3446	C—H_3 (50), C—H_2 (49)
	ν_2	3368	C—H_1 (98)
	ν_3	3315	C—H_3 (49), C—H_2 (49)
	ν_4	1636	C=C (44), C=C—H_2 (23), C=C—H_1 (14), C=C—H_3 (14)
	ν_5	1506	C=C—H_1 (43), C=C—H_3 (32), C=C (10), C—Cl (9), C=C—H_2 (6)
	ν_6	1355	C=C (39), C=C—H_1 (39), C=C—H_2 (16)
	ν_7	1151	C=C—H_2 (40), C=CH_3 (36), C—Cl (11), C=C—Cl (7), C=C—H_1 (6)
	ν_8	872	C—Cl (59), C=C—H_3 (17), C=C—H_2 (13), C=C—H_1 (5)
	ν_9	423	C=C—Cl (69), C=C—H_1 (16), C=C—H_3 (6), C=C—H_2 (6)

[a] The values of the PED (%) over 5% are listed
[b] The observed vibrational frequencies of the ground state are as follows: 3121 (ν_1), 3086 (ν_2), 3030 (ν_3), 1608 (ν_4), 1369 (ν_5), 1279 (ν_6), 1030 (ν_7), 720 (ν_8), and 395 (ν_9) cm^{-1} (Ref. [15])

Table 5. Vibrational frequencies (cm^{-1}) and (PED) of C_2HF_3[a]

State	Mode	Vibrational frequency	PED (%)
$^1A'$	ν_1	3448	C—H (99)
	ν_2	2041	C=C (71), C—F_1 (8), C—F_3 (7), C—F_2 (6)
	ν_3	1521	C—F_1 (30), C=C—H (25), C—F_2 (18), C=C—F_2 (13), C=C—F_1 (9)
	ν_4	1401	C=C—H (43), C—F_2 (38), C—F_3 (12)
	ν_5	1276	C—F_3 (70), C=C—F_2 (9), C=C —F_3 (7), C=C—H (6)
	ν_6	1029	C—F_1 (38), C=C (16), C—F_2 (13), C=C—F_3 (13), C=C—H (12), C=C—F_1 (5),
	ν_7	683	C=C—F_1 (46), C=C—F_3 (30), C—F_2 (12)
	ν_8	530	C=C—F_2 (83), C=C (6), C—F_3 (6)
	ν_9	242	C=C—F_1 (34), C=C—F_3 (29), C=C—F_2 (24), C=C—H (13)
$^2A''$	ν_1	3399	C—H (99)
	ν_2	1855	C=C (47), C—F_3 (20), C—F_2 (11), C—F_1 (9), C=C—H (9), C=C—F_1 (5)
	ν_3	1735	C—F_1 (41), C—F_2 (32), C=C—F_2 (10), C=C—F_1 (8), C=C—H (6)
	ν_4	1502	C—F_3 (35), C=C—H (29), C—F_2 (22), C—F_1 (6)
	ν_5	1358	C=C—H (45), C—F_3 (40), C=C—F_3 (6)
	ν_6	1047	C=C (31), C—F_1 (26), C=C—F_3 (13), C=C—H (13), C—F_2 (11)
	ν_7	707	C=C—F_1 (51), C=C—F_3 (33), C—F_2 (9), C=C—H (6)
	ν_8	538	C=C—F_2 (74), C=C (12), C=C—F_3 (8),
	ν_9	255	C=C—F_1 (36), C=C—F_2 (27), C=C—F_3 (26), C=C—H (11)

[a] The values of the PED (%) over 5% are listed

characterized by using the conventional potential energy distribution [14].

Theoretical intensity curves of C_2H_3F, C_2H_3Cl, C_2HF_3, and C_2HCl_3 with half-widths of 0.08 eV are compared with the observed photoelectron spectra in Fig. 1–4. Each theoretical intensity curve closely reproduces the photoelectron spectrum. Figures 5–8 indicate more resolved vibrational structure of the theoretical intensity curves with half-widths of 0.02 eV. An interpretation of each vibrational structure is given in Tables 7–10.

3.1 Vinylfluoride

The vibrational structure of the theoretical intensity curve is illustrated in Fig. 5. The assignment of the vibrational structure is given in Table 7. The first peak at 9.60 eV corresponds to the 0-0 transition. There are two main vibrational progressions of A and B. Overlap of the progressions of A and B dominates the form of the spectrum of Fig. 5. The vibrational progression A of $n\nu_4$ (n = 0–4) has strong intensity. The vibrational progression of B of $n\nu_4 + \nu_7$ (n = 0–3) and $n\nu_4 + \nu_6$

Table 6. Vibrational frequencies (cm^{-1}) and PED of C_2HCl_3[a]

State	Mode	Vibrational frequency[b]	PED (%)
$^1A''$	ν_1	3416	C—H (99)
	ν_2	1834	C=C—Cl_2 (83), C=C—H (5)
	ν_3	1362	C=C—H (86)
	ν_4	1014	C—Cl_2 (24), C=C—Cl_1 (22), C—Cl_1 (20), C=C—Cl_2 (18), C=C—Cl_3 (13)
	ν_5	897	C—Cl_3 (68), C—Cl_2 (20), C=C—Cl_2 (6), C=C—Cl_3 (5)
	ν_6	673	C—Cl_1 (53), C=C—Cl_3 (20), C=C—Cl_1 (12), C—Cl_2 (8)
	ν_7	412	C=C—Cl_1 (27), C—Cl_2 (27), C=C—Cl_3 (22), C—Cl_3 (15)
	ν_8	294	C=C—Cl_2 (83), C—Cl_3 (7), C=C—Cl_1 (6)
	ν_9	183	C=C—Cl_1 (38), C=C—Cl_3 (33), C=C—Cl_2 (20), C=C—H (8)
$^2A''$	ν_1	3379	C—H (99)
	ν_2	1583	C=C (61), C=C—H (21), C—Cl_3 (9)
	ν_3	1391	C=C—H (66), C=C (13), C—Cl_1 (10), C=C—Cl_2 (6)
	ν_4	1120	C—Cl_2 (32), C—Cl_1 (23), C=C—Cl_1 (18), C=C—Cl_2 (14), C=C—Cl_3 (11)
	ν_5	977	C—Cl_3 (68), C—Cl_2 (16), C=C—Cl_2 (7), C=C—Cl_3 (7)
	ν_6	694	C—Cl_1 (47), C=C—Cl_3 (23), C=C—Cl_1 (10), C—Cl_2 (9), C=C—Cl_2 (7)
	ν_7	431	C=C—Cl_3 (31), C=C—Cl_1 (29), C—Cl_2 (22), C—Cl_3 (9)
	ν_8	311	C=C—Cl_2 (79), C—Cl_3 (9), C—Cl_1 (5)
	ν_9	193	C=C—Cl_1 (45), C=C—Cl_2 (29), C=C—Cl_3 (22), C=C—H (5)

[a] The values of the PED (%) over 5% are listed

[b] The observed vibrational frequencies of the ground state are as follows: 3096 (ν_1), 1590 (ν_2), 1250 (ν_3), 850 (ν_4), 633 (ν_5), 452 (ν_6), 381 (ν_7), 272 (ν_8), and 169 (ν_9) cm^{-1} (Ref. [15])

(n = 0–3) has medium intensity. The ν_4 mode contributes to all progressions. Table 3 reveals that the character of ν_4 ($^2A''$ state) is a mixture of the C=C stretching, C—F stretching, and C=C—H bending motions. Table 11 gives the magnitude of the change in the geometry upon ionization and the classical half-amplitude of the zero-point vibrational level. This table helps us to understand the effect of the vibrational excitation of each mode on intensity in connection with the change in the geometry upon ionization. Vibrational excitation of ν_4 contributes to the intensity of the band. This situation is ascribed to the geometrical changes upon ionization. Table 11 reveals that the magnitudes of the geometrical changes in the C=C and C—F bond lengths are twice as large as the classical half-amplitudes of the C=C and C—F stretching motions. The magnitudes of the changes of the other geometrical parameters are smaller than the classical half-amplitudes. The C=C bond lengthens and the C—F bond shortens. For ν_4 the overlap of the C—F and C=C stretching motions is out of phase, which is consistent with the phase of the geometrical change upon ionization. Therefore, it can be said that the vibrational progression of $n\nu_4$ has strong intensity. The ν_6 and ν_7 modes have the amplitude of the C=C and C—F stretching motions, respectively. Thus, vibrational excitations of the ν_6 and ν_7 modes also contribute to the intensity.

3.2 Vinylchloride

The vibrational structure of the theoretical intensity curve is illustrated in Fig. 6. The assignment of the vibrational structure is given in Table 8. The first peak at 9.41 eV corresponds to the 0-0 transition. The vibrational excitations of ν_4, ν_5, ν_6, ν_7, and ν_8 contribute the to the intensity. The vibrational excitation of ν_4 has strong intensity. The character of ν_4 is a mixture of the C=C stretching and C=C—H bending motions (see Table 4).

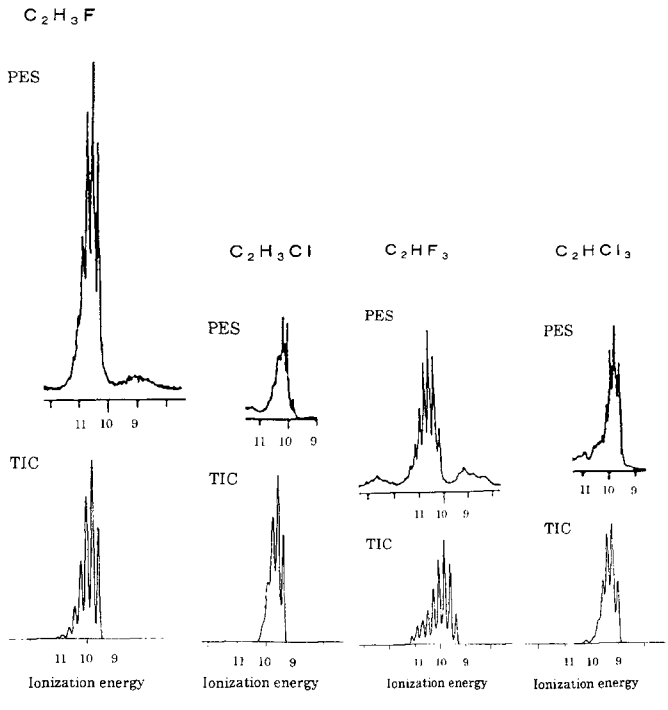

Fig. 1. Theoretical intensity curve (*TIC*) and photoelectron spectrum (*PES*) of vinyl fluoride [3]. Band-width: 0.08 eV

Fig. 2. TIC and PES of vinyl chloride [4]. Band-width: 0.08 eV

Fig. 3. TIC and PES of trifluoroethylene [3]. Band-width: 0.08 eV

Fig. 4. TIC and PES of trichloroethylene [4]. Band-width: 0.08 eV

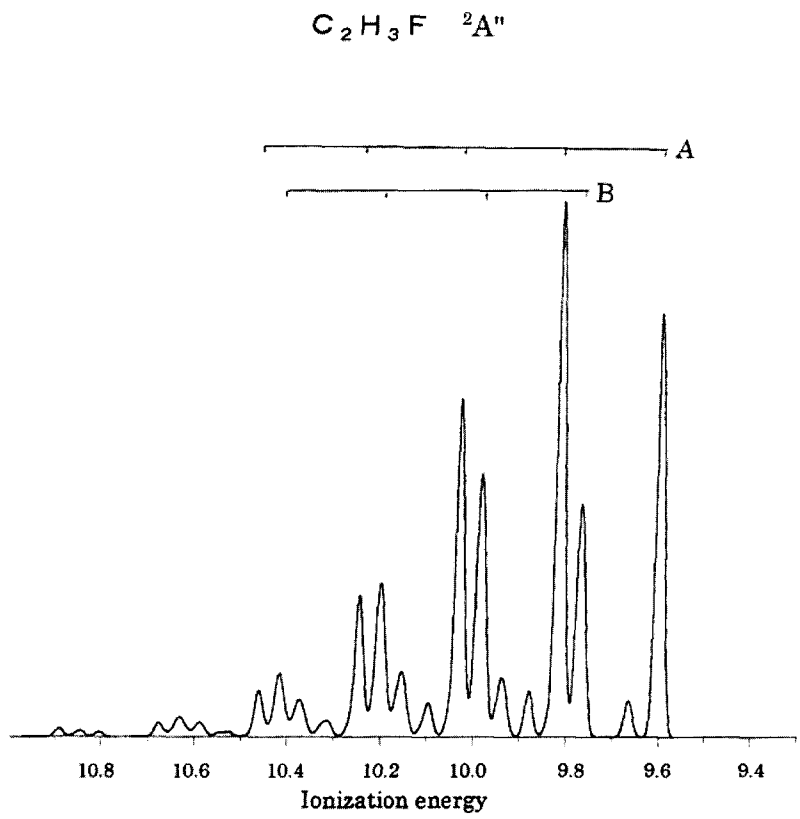

Fig. 5. Theoretical intensity curve of the $^2A''$ state of vinyl fluoride. Band-width: 0.02 eV

Table 11 reveals that the geometrical changes in the C=C and C—Cl bond lengths alone are twice as large as the classical half-amplitudes of the C=C and C—Cl stretching motions. The C=C bond lengthens and the C—Cl bond shortens. Although the ν_2 mode is characterized as a mixture of the C=C stretching and the C=C—H bending mode, it has some amplitude in the C—Cl stretching motion (see Table 11). The overlap of the C=C and C—Cl stretching motions is out of phase, which is consistent with the phase of the changes in the C=C and C—Cl bond lengths. Thus, vibrational excitation of ν_4 has strong intensity. The ν_5 mode is also an out-of-phase overlap mode of the C=C and C—Cl stretching motions. The ν_6, ν_7, and ν_8 modes have amplitudes of the C=C or C—Cl stretching motions. Therefore, vibrational excitations of the ν_5, ν_6, ν_7, and ν_8 modes also contribute to the intensity.

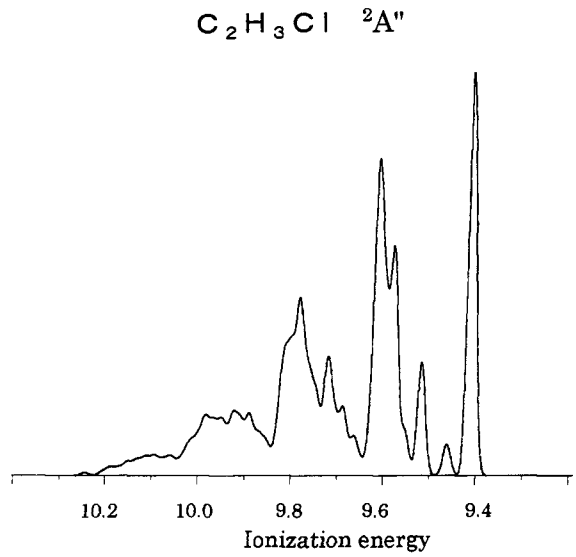

Fig. 6. Theoretical intensity curve of the $^2A''$ state of vinyl chloride. Band-width: 0.02 eV

3.3 Trifluoroethylene

The vibrational structure of the theoretical intensity curve is illustrated in Fig. 7. The assignment of the vibrational structure is given in Table 9. The first peak at 9.36 eV corresponds to the 0-0 transition. The vibrational progression of $n\nu_2$ (n = 0–6) dominates the form of spectrum. The vibrational progressions of $n\nu_2 + \nu_4$ (n = 0–3), $n\nu_2 + \nu_7$ (n = 0–3), and $n\nu_2 + \nu_9$ (n = 0–3) with weak intensity also contribute to the spectrum. The ν_2 mode contributes to all progressions. The character of ν_2 is a mixture of the C=C and C—F stretching motions (see Table 5). Higher vibrational excitation of ν_2 contributes to the intensity. This situation is ascribed to the geometrical change upon ionization. Table 12 indicates that the geometrical changes in the C=C and C—F bond lengths are larger than the classical half-amplitudes of the C=C and C—F stretching motions. The C=C bond lengthens and the C—F bond shortens. The ν_2 mode has amplitudes in the C=C and C—F stretching motions. The overlap of the two motions is out of phase, which is

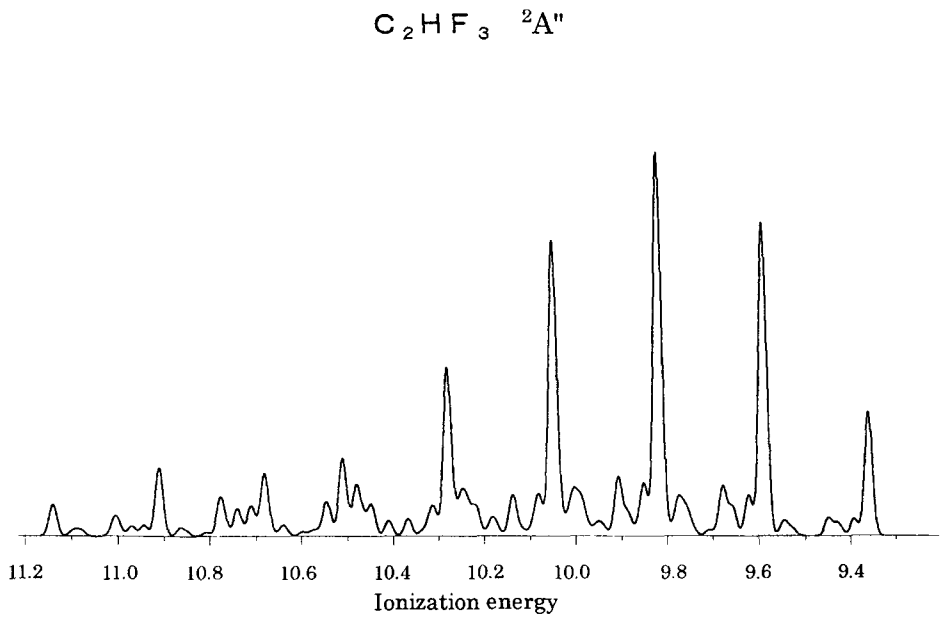

Fig. 7. Theoretical intensity curve of the $^2A''$ state of trifluoroethylene. Band-width: 0.02 eV

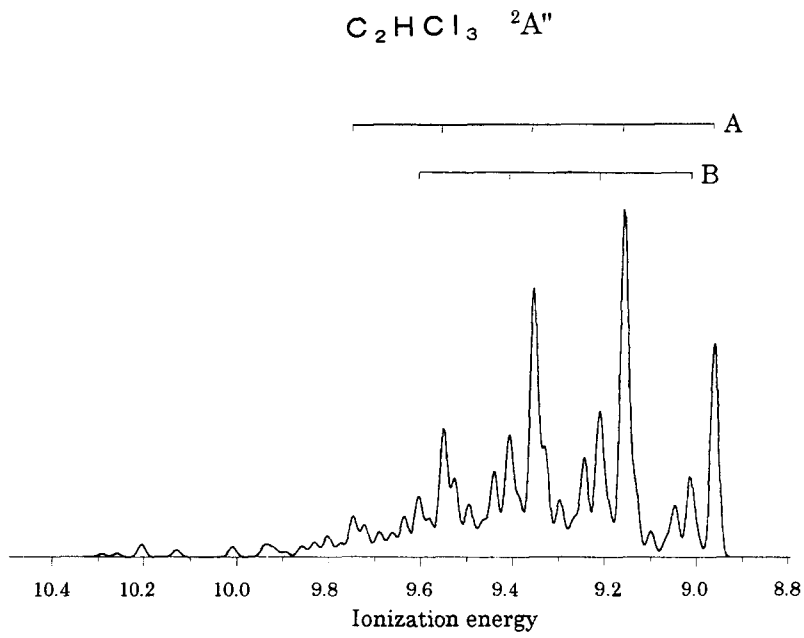

Fig. 8. Theoretical intensity curve of the $^2A''$ state of trichloroethylene. Band-width: 0.02 eV

consistent with the changes in the C=C and C—Cl bond lengths. Therefore, vibrational excitation of ν_2 has strong intensity.

3.4 Trichloroethylene

The vibrational structure of the theoretical intensity curve is illustrated in Fig. 8. The assignment of the vibrational structure is given in Table 10. The first peak at 8.96 eV corresponds to the 0-0 transition. The vibrational progression A of $n\nu_2$ (n = 0–4) has strong intensity. The vibrational progression B of $n\nu_2 + \nu_7$ (n = 0–3) has medium intensity. The other vibrational levels of $n\nu_2 + \nu_3$ (n = 0–2) and $n\nu_2 + \nu_6$ (n = 0–3) also contribute to the intensity. The ν_2 mode contributes to all progressions. The character of ν_2 is the C=C stretching mode (see Table 6). The contribution of higher vibrational excitation of ν_2 is connected to the geometrical change upon ionization. Table 12 reveals that the geometrical changes in the C=C and C—Cl bond lengths alone are larger than the classical half-amplitudes of the C=C and C—Cl stretching motions. The C=C bond lengthens and the C—Cl bond shortens. Although the character of ν_2 is the C=C stretching mode, the ν_2 mode has some amplitude in the C—Cl sretching motion (see Table 12). The phase of the C=C and C—Cl stretching motions is consistent with the phase of the change in the C=C and C—Cl bond lengths. Therefore, it can be said that vibrational excitation of ν_2

Table 7. Vibrational levels of the $^2A''$ state of C_2H_3F[a]

IE	Progressions		Other levels
	A	B	
9.60	0 (s)		
9.66			ν_9 (w)
9.77		ν_7 (m), ν_6 (m)	
9.81	ν_4 (s)		
9.88			$\nu_4+\nu_9$ (w)
9.93			$2\nu_7$ (w)
9.94			$\nu_6+\nu_7$ (w)
9.98–9.99		$\nu_4+\nu_7$ (m), $\nu_4+\nu_6$ (m)	
10.03	$2\nu_4$ (s)		
10.16			$\nu_4+\nu_6+\nu_7$ (w)
10.20–10.21		$2\nu_4+\nu_7$ (m), $2\nu_4+\nu_6$ (w)	
10.25	$3\nu_4$ (m)		
10.41–10.42		$3\nu_4+\nu_7$ (w), $3\nu_4+\nu_6$ (w)	
10.46	$4\nu_4$ (w)		

[a] Intensity is classified into strong (*s*), medium (*m*), or weak (*w*) according to the magnitude of the Franck–Condon Factor (FCF) as follows: s: 0.18 > FCF > 0.10, m : 0.07 > FCF > 0.03, or w: 0.03 > FCF > 0.01

Table 8. Vibrational levels of the $^2A''$ state of C_2H_3Cl[a]

IE	Strong	Medium	Weak
9.41	0 (s)		
9.46			ν_9 (w)
9.52		ν_8 (m)	
9.55			ν_7 (w)
9.58	ν_6 (s)		
9.60		ν_5 (m)	
9.61	ν_4 (s)		
9.69			$\nu_6+\nu_8$ (w)
9.70			$\nu_5+\nu_8$ (w)
9.72			$\nu_4+\nu_8$ (w)
9.75			$2\nu_6$ (w)
9.76			$\nu_4+\nu_7$ (w), $\nu_5+\nu_6$ (w)
9.78		$\nu_4+\nu_6$ (m)	
9.80		$\nu_4+\nu_5$ (m)	
9.82			$2\nu_4$ (w)
9.89			$\nu_4+\nu_6+\nu_8$ (w)
9.91			$\nu_4+\nu_5+\nu_8$ (w)
9.97			$\nu_4+\nu_5+\nu_6$ (w)

[a] Intensity is classified into s, m, or w according to the magnitude of the FCF as follows: s: 0.14 > FCF > 0.07, m: 0.05 > FCF > 0.03, or w: 0.03 > FCF > 0.01

Table 9. Vibrational levels of the $^2A''$ state of $C_2HF^a{}_3$

IE	Main progression	Others
9.36	0(m)	
9.59	ν_2 (s)	
9.62		$\nu_2+\nu_9$ (w)
9.68		$\nu_2+\nu_7$ (w)
9.78		$\nu_2+\nu_4$ (w)
9.82	$2\nu_2$ (s)	
9.85		$2\nu_2+\nu_9$ (w)
9.91		$2\nu_2+\nu_7$ (w)
9.99		$2\nu_2+\nu_5$ (w)
10.01		$2\nu_2+\nu_4$ (w)
10.05	$3\nu_2$ (s)	
10.08		$3\nu_2+\nu_9$ (w)
10.14		$3\nu_2+\nu_7$ (w)
10.28	$4\nu_2$ (m)	
10.48		$4\nu_2+3\nu_9$ (w)
10.51	$5\nu_2$ (w)	
10.68		$3\nu_2+2\nu_3+3\nu_8$ (w)
10.78		$4\nu_2+2\nu_3+\nu_8$ (w)
10.91		$4\nu_2+2\nu_3+3\nu_8$ (w)

[a] Intensity is classified into s, m, or w according to the magnitude of the FCF as follows: s: 0.13 > FCF > 0.09, m: 0.06 > FCF > 0.03, or w: 0.03 > FCF > 0.01

Table 10. Vibrational levels of the $^2A''$ state of C_2HCl_3[a]

IE	Progression		Others
	A	B	
8.96	0 (m)		
9.01		ν_7 (w)	
9.05			ν_6 (w)
9.13			ν_3 (w)
9.16	ν_2 (s)		
9.21		$\nu_2+\nu_7$ (m)	
9.24			$\nu_2+\nu_6$ (w)
9.30			$\nu_2+\nu_6+\nu_7$ (w)
9.33			$\nu_2+\nu_3$ (m)
9.35	$2\nu_2$ (s)		
9.38			$\nu_2+\nu_3+\nu_7$ (w)
9.41		$2\nu_2+\nu_7$ (m)	
9.44			$2\nu_2+\nu_6$ (w)
9.52			$2\nu_2+\nu_3$ (w)
9.55	$3\nu_2$ (m)		
9.60		$3\nu_2+\nu_7$ (w)	
9.63			$3\nu_2+\nu_6$ (w)
9.74	$4\nu_2$ (w)		

[a] Intensity is classified into s, m, or w according to the magnitude of the FCF as follows: s:0.12 > FCF > 0.07, m:0.05 > FCF > 0.03, or w:0.03 > FCF > 0.01

mainly contributes to the intensity. The ν_3, ν_6, and ν_7 modes have amplitudes of the C=C and C—Cl stretching motions. Therefore, excitations of the ν_3, ν_6, and ν_7 modes also contribute to the intensity.

4 Conclusion

The equilibrium molecular structures and vibrational frequencies were calculated for the ground and the first ionic states. We have obtained the theoretical intensity curve by using the FCFs. All theoretical intensity curves reproduce the observed photoelectron spectra closely.

For all molecules the C=C bond lengthens and the C—X (X = F or Cl) bond shortens upon ionization. This situation is connected with the fact that vibrational excitation of the out-of-phase overlap mode of the C=C and C—X stretching motions dominates the form of the spectrum

Acknowledgement. Computation was carried out on HITAC M-680H systems at the Center for Information Processing Education of Hokkaido University.

Table 11. Magnitude of the change in the geometry upon ionization and the classical half-amplitude[a]

	C=C	C–X[b]	C–H_1	C–H_2	C– H_3	C= C–X[b]	C=C–H_1	C=C–H_2	C=C–H_3
C_2H_3F									
ΔR^c	0.090	−0.076	0.006	0.003	0.002	−2.9	−0.8	−1.5	−0.1
ν_1	−0.001	0.000	0.005	−0.069	0.079	−0.4	0.4	0.7	−0.6
ν_2	−0.006	−0.004	0.103	0.012	0.003	0.7	−0.3	−0.3	0.4
ν_3	−0.006	0.001	−0.011	0.077	0.067	−0.0	0.0	0.3	0.3
ν_4	−0.041	0.035	−0.002	−0.002	−0.002	−0.0	5.1	3.0	0.6
ν_5	−0.010	−0.021	−0.002	−0.001	−0.001	0.7	−2.3	3.9	6.5
ν_6	0.002	−0.030	−0.002	0.000	−0.001	1.2	5.3	−1.4	0.1
ν_7	0.038	0.011	0.005	0.003	0.001	−2.4	3.5	5.1	−1.7
ν_8	0.018	0.016	0.000	0.001	0.002	1.0	1.0	−5.6	6.2
ν_9	0.005	0.001	0.000	0.000	0.001	4.5	−3.2	3.0	−2.7
C_2H_3Cl									
ΔR^c	0.087	−0.097	0.006	0.002	0.001	−1.0	−2.8	−1.3	0.1
ν_1	0.000	0.000	0.006	−0.073	0.074	−0.4	0.4	0.7	0.7
ν_2	−0.006	−0.004	0.103	0.012	0.003	0.6	−0.3	−0.3	0.4
ν_3	−0.007	0.001	−0.011	0.072	0.072	−0.1	0.1	0.3	0.3
ν_4	−0.042	0.017	−0.003	−0.002	−0.002	0.2	3.5	4.8	3.6
ν_5	−0.019	0.021	−0.001	−0.001	−0.001	−0.3	5.7	−2.2	5.3
ν_6	0.036	−0.005	0.002	0.003	0.001	−1.4	5.3	3.7	1.3
ν_7	−0.002	0.024	0.002	0.001	0.000	−2.1	−2.2	6.1	5.8
ν_8	0.012	0.046	0.002	0.001	0.001	−1.2	1.2	−2.9	3.3
ν_9	0.004	0.005	0.000	0.000	0.001	4.3	−2.4	1.6	1.6

[a] Bond lenghts in angstroms, angles in degress
[b] X = F or Cl
[c] ΔR is the magnitude of the change in the geometry

Table 12. Magnitude of the change in the geometry upon ionization and the classical half-amplitude[a]

	C=C	C–X_1^b	C–X_2[b]	C–X_3[b]	C–H	C=C–X_1^b	C=C–X_2[b]	C=C–X_3[b]	C=C–H
C_2HF_3									
ΔR^c	0.098	−0.058	−0.061	−0.064	0.007	−3.3	−2.2	−3.4	−0.2
ν_1	−0.005	0.000	0.000	−0.005	0.103	−0.3	0.3	0.6	−0.3
ν_2	−0.048	0.018	0.020	0.028	−0.001	1.7	0.5	0.1	3.1
ν_3	0.004	−0.043	0.038	0.002	0.001	2.3	−2.5	−1.6	2.7
ν_4	0.012	−0.013	−0.026	0.034	0.002	−0.4	−1.5	−0.5	5.1
ν_5	−0.007	0.005	−0.002	−0.030	−0.003	−0.8	1.1	1.6	5.2
ν_6	0.029	0.023	0.015	0.005	0.003	0.7	−0.9	−2.2	2.8
ν_7	−0.001	−0.003	−0.011	−0.004	0.001	3.2	−0.3	−2.9	1.5
ν_8	0.013	−0.003	0.002	0.007	0.000	−0.4	3.2	1.2	−0.3
ν_9	0.002	0.000	0.001	−0.002	0.000	2.7	−2.4	2.6	−2.1
C_2HCl_3									
ΔR^c	0.093	−0.055	−0.064	−0.072	0.005	−2.3	−2.0	−0.6	−2.1
ν_1	−0.005	0.000	0.000	−0.004	0.104	−0.3	0.3	0.6	−0.3
ν_2	−0.054	0.012	0.016	0.025	−0.003	1.3	0.2	0.2	4.6
ν_3	0.024	−0.025	0.000	0.004	0.001	0.6	−1.8	−1.2	7.6
ν_4	−0.002	−0.039	0.046	0.009	0.001	3.0	−2.7	−2.5	−1.0
ν_5	0.008	−0.001	−0.025	0.051	0.002	0.3	−1.5	−1.5	0.2
ν_6	−0.012	−0.037	−0.016	−0.003	−0.002	−1.5	0.0	2.4	−1.3
ν_7	0.006	0.003	0.020	0.013	0.000	−2.0	0.5	2.1	−0.8
ν_8	0.004	−0.007	0.000	0.009	0.000	0.5	2.4	0.2	−0.1
ν_9	0.000	0.000	0.001	0.001	0.000	2.1	−1.7	1.5	−0.9

[a] Bond lengths in angstrom, angles in degrees
[b] X = F or Cl
[c] ΔR is the magnitude of the change in the geometry

References

1. Lake RF, Thompson H (1970) Proc R Soc Lond Ser A 315:323
2. Sell JA, Kuppermann A (1979) J Chem Phys 71:4703
3. Bieri G, Åsbrink L, Niessen WV (1981) J Electron Spectrosc Relat Phenom 23:281
4. Niessen WV, Åsbrink L, Bieri G (1982) J Electron Spectrosc Relat Phenom 26:173
5. Kimura K, Katsumata S, Achiba Y, Yamazaki T, Iwata S (1981) Handbook of HeI photoelectron spectra of fundamental organic molecules. Halsted, New York
6. Heaton MM, El-Talbi MR (1986) J Chem Phys 85:7198
7. Tatewaki H, Huzinaga S (1980) J Comput Chem 1:205
8. Sakai Y, Tatewaki H, Huzinaga S (1981) J Comput Chem 2:100
9. Takeshita K (1987) J Chem Phys 86:329

10. Takeshita K, Sasaki F (1981) Library program at the Hokkaido University Computing Center (in Japanese). GRAMOL includes the Program JAMOL3 of the RHF calculation written by Kashiwagi H, Takada T, Miyoshi E, Obara S for the Library program at the Hokkaido University Computing Center 1977 (in Japanese)
11. Lengsfield BH III (1980) J Chem Phys 73:382
12. Liu B, Yosimine M (1981) J Chem Phys 74:612
13. Lengsfield BH III, Liu B (1981) J Chem Phys 75:478
14. Morino Y, Kuchitsu K (1952) J Chem Phys 21:1809
15. Herzberg G (1966) Molecular spectra and molecular structure, part III. van Nostrand, New York